2020

Detection of Point Mutations Conferring Gentamicin Resistance in Escherichia coli using a Split-G4 Probe

Michael J. Greenberg
University of Central Florida

DETECTION OF POINT MUTATIONS CONFERRING GENTAMICIN RESISTANCE IN *ESCHERICHIA COLI* USING A SPLIT-G4 PROBE

by

MICHAEL GREENBERG

A thesis submitted in partial fulfillment of the requirements
for the Interdisciplinary Honors Thesis in Chemistry
in the College of Sciences
and in the Burnett Honors College
at the University of Central Florida
Orlando, Florida

Fall, 2020

Thesis Chair: Yulia Gerasimova, Ph.D.

ABSTRACT

The objective of this project was to develop a DNA hybridization sensor that can detect the presence of *E. coli* and reveal its resistance to the drug gentamicin. This probe will enable rapid and user-friendly diagnostics of *E. coli* infections and analysis of bacterial gentamicin-susceptibility profile by interrogation of a fragment of *E. coli* 16S rRNA bearing a substitution in the gentamicin-resistant cells. The sensor is promising for the point-of-care use to provide a timely UTI diagnostic solution. A quick diagnosis of *E. coli* infection and antibiotic resistance is crucial for treatment. To design a hybridization probe, we proposed a split approach for target interrogation and catalytic activity of a peroxidase-like deoxyribozyme (PDz) as a signal reporter. PDz contains a series of guanine residues in a strand and has been shown to form a parallel guanine-quadruplex (G4). This G4, with the addition of a hemin cofactor, catalyzes the reaction similar to that of horseradish peroxidase. If a colorless organic indicator is added to the G4-PDz-hemin containing solution and mixed H_2O_2, a colored oxidation product is formed (e.g., a dark blue/green). The color change reports the presence of the catalytically active G4, which occurs only when the nucleotide sequence of the target is a perfect match. When the target is not a perfect match, for example, in the case of the drug-causing nucleotide substitution, the G4 does not form, and there is no color change. The probes tested in this paper show promising results of such a sensor by being able to catalyze the described colorimetric reaction to generate a strong signal in the presence of a "gentamicin-susceptible" target and show selectivity against the "gentamicin-resistant" target.

TABLE OF CONTENTS

List of Figures

List of Tables

LIST OF MEDIA/ABBREVIATIONS/ACRONYMS

1. UTI = Urinary tract infection
2. PDz = Peroxidase-like deoxyribozyme
3. sPDz = split peroxidase-like deoxyribozyme
4. ABTS = 2,2′-Azino-bis (3-ethylbenzthiazoline-6-sulfonic acid)
5. 1X TAE = Tris-acetate-EDTA buffer (40 mM Tris, 20 mM acetate, 1 mM EDTA disodium salt dehydrate)
6. PCR = Polymerase Chain Reaction
7. G4 = G-quadruplex/Guanine quadruplex
8. LB = Luria-Bertani media
9. WT = Wild type
10. SF = Selectivity Factor
11. NTC = No target control

INTRODUCTION

Urinary tract infections (UTI) are a universal health care issue. *Escherichia coli* (*E. coli*) is the cause of 75-90% of urinary tract infections.[1] Untreated UTIs can develop into diseases such as pyelonephritis, which is when the bacteria spread from the bladder to the kidneys, causing more severe symptoms, such as back/flank pain and vomiting.[2] With around 400,000 cases of UTIs leading to hospitalization each year, the total healthcare cost associated with UTI has been estimated to be $3.5 billion annually in the United States.[3-4] Timely diagnostics of UTI with more precise treatment have the potential to reduce the number of victims and annual cost.

A conventional approach for UTI diagnostics, apart from the one based on symptoms, relies on culturing the cells, which takes 24 hours or more for growth.[5] This wait period for confirmation delays treatment initiation; rapid treatment is crucial to prevent the development of symptoms and halt the spread of the infection. Another limitation of current diagnostics is that these methods have an error rate of about 33%.[5] This means 1/3 of patients with a UTI may not be correctly diagnosed the first time and, therefore, may go untreated, leading to other potential health issues.

The treatment and control over UTI are further complicated by the fact that *E. coli* develops resistance to the antibiotics generally prescribed for bacterial UTI treatment. For example, one of the most effective first-line antibiotics against UTI-causing bacteria, such as *E. coli*, is an aminoglycoside antibiotic gentamicin. [6-7] The mechanism of gentamicin's action involves binding at helix 44 (A-site) of the 16S rRNA component of the 30S ribosomal subunit, thereby preventing the correction of incorrectly bound aminoacyl-tRNA, which causes bacteria to synthesize proteins

with wrong primary structure.[7-8] One of the mechanisms bacteria develop resistance to gentamicin is through modification of the sequence of 16S rRNA by acquiring point-mutations in the *rrs* gene encoding 16S rRNA.[7-8] The substitution of guanine at the position nt1408 or adenine at nt1406 of 16S rRNA with guanine prevents interaction of the drug with the A-site of the bacterial ribosome and the cell can grow unimpeded.[6,10] This substitution that is tightly linked to gentamicin resistance occurs in about 12.9% of *E. coli* cells.[9]

Differentiation between wild type (T1406) and mutant (T1406A) genotypes constitutes the grounds for molecular gentamicin-susceptibility testing. Current methods analyzing the molecular basis of antibiotic-resistant genes involve real-time Polymerase Chain Reaction (PCR).[11] This technique has limited validity due to the increased number of false positives, while having a run time of about an hour and increasing the cost of running the test.[11] RNA mutations can be detectable using the enzyme Reverse-Transcriptase followed by rounds of PCR amplification in real-time.[1] PCR techniques for discrimination between point mutations may require a melting temperature profile at the end of the amplification. This melting temperature profile can only be done with qPCR instruments, which not hospitals or private clinics have due to expense. PCR, therefore, cannot be used to diagnose all bacteriuria as it would be inadequate when it comes to showing presence of antibiotic-resistant bacteria or when there are no bacteria.[11-12] The use of a TaqMan probe for genotyping samples requires the use of Thermocyclers and thermo-stable DNA polymerases, which are not readily available in clinic settings. Other techniques often utilize probes following PCR, adding time to the point of complete diagnosis. The most ideal tool for detection of mutations will be expedient, easy to use, and accurate, which is exactly how the proposed method for detection will perform.

We proposed a method for molecular detection of the presence and antibiotic resistance in *E. coli* that involves using a split hybridization DNA probe that exhibits enzymatic activity capable of a colorimetric assay. Similar probes have been tested previously for the detection of non-tuberculosis mycobacteria, zika virus, rifampin resistant mycobacterium tuberculosis and others.[13-15] It has been demonstrated that the probes are very sensitive to single nucleotide substitutions.[13-17] Using this probe, the presence of an RNA target can be detected within 30 minutes or less at room temperature without the need of expensive instrumentation to monitor the signal, since the probe results in the color change of a solution in response to a specific target. Such instrument-free visualization makes it easy to read the test results, and for those reasons deliver the most optimal treatment to patients.

To design a hybridization probe, we used a split approach for target interrogation and catalytic activity of a peroxidase-like deoxyribozyme (PDz) as a signal reporter. The "Split" approach uses two probes each with G4 forming arms and each with analyte-binding arms that are complementary to a target. Upon hybridization of the analyte-binding arms to the target, the G4 forming arms are coordinated together to fold into the G4 (Figure 1). PDz contains a series of guanine residues in a strand and has been shown to form a parallel guanine-quadruplex (G4). This G4, with the addition of a hemin cofactor, has been found to catalyze the reaction similar to that of horseradish peroxidase.[16] If a colorless organic indicator (e.g., $ABTS^{2-}$) is added to the G4-PDz-hemin containing solution and mixed hydrogen peroxide, a colored oxidation product is formed (e.g., a dark blue/green $ABTS^{\cdot-}$). The color change reports the presence of the catalytically active G4 (Figure 2).

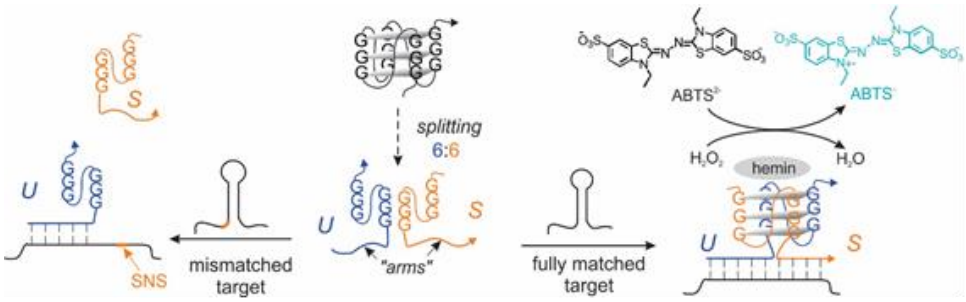

Figure 1: Design and mechanism of action of a colorimetric split PDz probe (sPDz).[17]

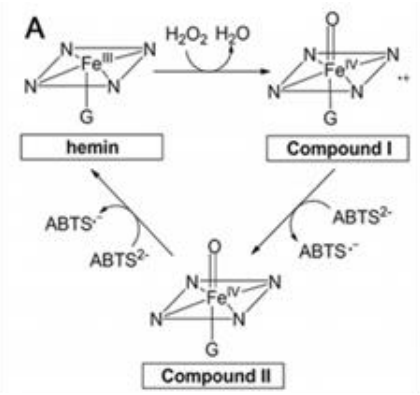

Figure 2: Mechanism of G4-PDz-hemin catalysis of a peroxidation reaction.[18]

The catalytic cycle of ABTS peroxidation by the G4-PDz-hemin complex is depicted in Figure 2. The reduced form of hemin (top left) can reduce H_2O_2 into H_2O to generate Compound I. Compound I will now oxidize $ABTS^{2-}$ (colorless) into the colored product $ABTS^{\cdot-}$, which will generate Compound II. Compound II is capable of catalyzing another oxidation round to convert another molecule of $ABTS^{2-}$ into $ABTS^{\cdot-}$, which will regenerate the catalyst hemin, thereby producing two molecules of colored product per cycle of catalysis.[18] The increase in oxidized $ABTS^{\cdot-}$ molecules is positively correlated with absorbance of the solution. The reaction has the most significant absorbance values within 15 minutes of incubation and can be measured at 420 nm (absorbance of $ABTS^{\cdot-}$) on a spectrophotometer.

OBJECTIVE

The objective of this project is to develop and test a DNA hybridization probe that can detect the presence of *E. coli* and reveal its resistance to the drug gentamicin. This probe will enable rapid and user-friendly diagnostics of *E. coli* infections and analysis of bacterial gentamicin-susceptibility profile by interrogation of a fragment of *E. coli* 16S rRNA bearing an T1406A substitution in the gentamicin-resistant cells. The probe is promising for the point-of-care use to provide a timely UTI diagnostic solution. A quick diagnosis of *E. coli* infection and antibiotic resistance is crucial for quintessential treatment.

METHODOLOGY

Materials:

The DNA oligonucleotides were obtained from IDT Inc. (Coralville, IA, USA) and were not purified. The oligonucleotides were diluted with DNase free water to reach a final concentration of 100 µM stock solutions. H_2O_2 and ABTS were obtained from Sigma-Aldrich (St. Louis, MO, USA).

Procedures:

Colorimetric assay. Samples were prepared by mixing of the WT-S1 strand (1 µM), the WT-U1 (1 µM) with or without Blocking Element (1 µM) in a colorimetric buffer containing 50 mM HEPES-NaOH, pH 7.4, 50 mM $MgCl_2$, 20 mM KCl, 120 mM NaCl, 1% DMSO, and 0.03% Triton X-100 at 22°C. To some samples, the targets (1 µM), either the wild type or containing a point mutation at nt1406, were added. For color generation, hemin (0.375 µM), $ABTS^{2-}$ (1 mM) and H_2O_2 (1 mM) were added and incubated for 15 minutes to observe the change of the sample solutions into a dark blue-green color. To optimize the assay conditions, the colorimetric buffer was prepared at a pH of 6.8. In some experiments, the probe strands were annealed to the target by heating at 95 ºC for three minutes and slowly cooling to room temperature overnight prior to addition of hemin, $ABTS^{2-}$, and H_2O_2. The color intensity was measured using a Thermo Scientific

NanoDrop OneC UV-Vis Spectrophotometer (Waltham, MA, USA) at 420 nm. Tube images were captured using a cell phone camera immediately before measuring the samples' absorbance.

Extraction of total bacterial RNA.

E. coli cells were inoculated with a standard loop grown in two sets of 20 ml Luria-Bertani (LB) media for 24 hours at 37^{o}C in an attempt to keep the cells in the logarithmic growth phase. Following the incubation, the two sets were combined and pelleted by centrifugation at 16,000 rcf for 10 minutes at 4^{o}C. The supernatant was decanted, and the remaining cells were gently resuspended in 700 µL of nuclease free H_2O and 1 mg of lysozyme for 10 minutes. The solution was equally divided into two microcentrifuge tubes at 350 µL and an equal volume of Phenol-Chloroform was added in both and swirled. These microcentrifuge tubes were centrifuged at 16,000 rcf for 2 minutes at 4^{o}C and two distinct layers were formed: the aqueous layer and the organic layer. Because of the aromaticity of ribonucleic bases, the RNA was expected to separate into the organic layer, where proteins and other cellular components were more likely to be separated into the aqueous layer. The organic layer of each microcentrifuge tube was pipetted into a fresh microcentrifuge tube without disturbing the aqueous layer. Next, the samples were precipitated by adding 35 µL of 3 M sodium acetate, 1,000 µL of 100% ethanol, and 5 µL of glycogen 1 mg/ml to both samples and then stored at -70^{o}C for 10 minutes. Next, the samples were centrifuged at 16,000 rcf for 2 minutes at 4^{o}C to form a pellet and the supernatant was decanted. 500 µL of 70% ethanol was added to both samples and centrifuged once more at 16,000 rcf for 2 minutes at 4^{o}C. The steps were repeated by decanting the supernatant, adding 500 µL of 70% ethanol, and centrifuging once more and the supernatant was drained. The resultant precipitate was

resuspended in 20 µL of TE buffer at a pH of 8.1 each and the samples were labeled *E. coli* RNA 1 and 2 respectively. Next, an agarose gel was run to confirm the presence of the 16S ribosomal RNA and to calculate the concentration in the TE buffer.

The 0.8% agarose gel was prepared by suspending 0.4 g of agarose in 50 mL solution of 1X TAE buffer followed by boiling the suspension until the suspension is homogenous, and no agarose powder particles are visible. Once the solution cooled to 50^{o}C, 5 µL of 10,000X GelRed was added and swirled. Once mixed, the solution was poured into a horizontal casting tray with a 6-lane comb where the solution cooled into an agarose gel. 1X TAE buffer was poured over the container until the gel was covered. Solutions were prepared with 1.5 µL of nuclease free H_2O, 3 µL of 2X RNA Gel loading dye, and 1.5 µL of sample. Lane 1 contained the RiboRuler High-Range RNA Ladder as the sample, lane 2 and 3 each contained RNA from the samples suspended into the TE buffer. The negative terminal was plugged into the bottom of the gel and the positive terminal at the top. The machine was set to 80 V and run until the dye ran roughly two-thirds of the way down, and then taken to the GelDoc for visualization.

This sample was then precipitated by adding 3.5 µL of 3 M sodium acetate, 110 µL of 100% ethanol, and 5 µL of glycogen 1 mg/ml to both samples and then stored at -70^{o}C for 10 minutes. Next, the samples were centrifuged at 16,000 rcf for 2 minutes at 4^{o}C to form a pellet and the supernatant was decanted. 50 µL of 70% ethanol was added to both samples and centrifuged once more at 16,000 rcf for 2 minutes at 4^{o}C. The steps were repeated by decanting the supernatant, adding 50 µL of 70% ethanol, and centrifuging once more and the supernatant was drained. The reaction buffer was then prepared on top of this precipitate at 10 µL.

RESULTS

Design of the Split G4-PDz Probes Targeting E. coli 16S rRNA

In order to make the signal to be dependent on the presence of a nucleic acid target, the series of guanine nucleotides forming a G4 structure have been split between two strands of DNA to make a split PDz (sPDz) probe.[16] The sPDz probe has two strands, each strand containing a half of the G4-forming nucleotides, and a target-binding arm. One strand has a long "unwinding" target-binding arm that is complementary to both the wild type and mutant target; the second strand has a short "selective" segment that is complementary only to the wild type target (in the case of wild-type specific probes). The G4 structure is formed upon hybridization of the strands to the complementary target, and the G4 can bind to hemin for the peroxidase reaction (Figure 1). The probe was designed using the split-G4 approach because of the high selectivity that allows for differentiation between the wild-type 16S rRNA sequence and the sequence containing single-nucleotide substitutions conferring drug-resistance. Mutations in the fragment of the target that binds to the selective probe significantly reduces its ability to bind.[13-17] Therefore, the wild type target triggers a stronger signal, which can be clearly differentiated from the weak or no signal caused by the mutant analyte. This selectivity can help aid in diagnosis and treatment more specific to the strain of bacteria present.

We used a split G4 as a probe to interrogate a fragment of *E. coli* 16S rRNA, and also to differentiate between the wild type RNA sequence (gentamicin-susceptible phenotype) and mutant sequences with point mutations at nucleotide 1406 of the 16S rRNA, which has been correlated

with gentamicin resistance in *E. coli*.[9-10] In the design of a split peroxidase-like deoxyribozyme (sPDz) probe, strand U binds to the RNA target adjacent to strand S, which binds to the analyte containing the locations 1406 of the wild type (WT) sequence. When the mutation is present, the strength of the binding of the S strand is weaker because there are fewer complementary bases and the G4 reporter is not formed, ensuring the selectivity for the technique. The blocking strand, Strand B, binds upstream of the selective arm on the target. Because the blocking strand is so complementary to the target it helps undo the secondary structure of the 16S ribosomal, thereby increasing access for the hybridization of our probes to the target sequences. We also designed a sPDz probe specific for the mutant 16S rRNA sequence. Due to the split character of the probe, we only needed to adjust the sequence of strand S of the mutant-specific sPDz to be complementary to the mutation-containing fragment of 16S rRNA. By using both WT- and mutant-specific probes, it was possible to answer two questions at the same time: (1) whether or not *E. coli* has been accumulated in the biofluid samples; and (2) whether or not the bacterial species are susceptible to gentamicin. Alternatively, another probe that interrogates the sequence of *E. coli* 16S rRNA outside the fragment containing the mutation position (or 23S rRNA) can be used in combination with either WT or mutant-specific sPDz to provide the answer to these two questions. The sequences for the strands of sPDz probes are listed in Table 1.

In order to test and optimize the performance of the designed sPDz probes, synthetic 89-nt DNA sequences that correspond to the targeted fragment of 16S rRNA from *E. coli* were used as analytes. The sequences of the synthetic analytes are shown in Table 1. We expected that the WT-specific probe would bind to the WT analyte very well, but presence of T1406A substitution in the analyte would prevent the probes from binding, and therefore there would be no PDz formed to

catalyze the peroxidase reaction, as illustrated in Figure 1, left, so little to no colored product would form. The structure of the complex between the probe and WT analyte without the blocking strand is shown in Figure 3. The structure with the addition of the Blocking Element is shown in Figure 4 and the free energy of the complex is estimated to be -499.82 kJ/mol, which means this structure is very favorable. Nupack was used to calculate the structure and stability under the proposed conditions, but the tool is not capable of creating the G-quadruplex (https://www.nupack.org).[19] However, the G-quadruplex forming arms are visibly coordinated by complexing to the analyte.

Table 1: The sequences of the sPDz probe strands and analytes used in the project. [a]

Name	Sequence (5'→3')
WT	GTGAATACGTTCCCGGGCCTTGTACACACCGCCCGTCACACCATGGGAGTGGGTTGCAAAAGAAGTAGGTAGCTTAACCTTCGGGAGG
T1406A	GTGAATACGTTCCCGGGCCTTGTACACACCGCCCGACACACCATGGGAGTGGGTTGCAAAAGAAGTAGGTAGCTTAACCTTCGGGAGG
Blocking Element	GTGTACAAGGCCCGGGAACGTATTCACC
WT-S1	GGGTTGGGTGTGTGACG
WT-U1	GCTACCTACTTCTTTTGCAACCCACTCCCATGTGGGTTGGG
WT-S2	GGGTTGGGTGTGTGACG
WT-U2	CTACCTACTTCTTTTGCAACCCACTCCCATGTGGGTTGGG
WT-S3	GGGTTGGGTTGTGACGGG
WT-U3	CTACCTACTTCTTTTGCAACCCACTCCCATGGTGGGTTGGG
WT-slD2SA-1	*GGGT**TGG**GT*GTGTGACGG***CCA***
WT-slS2	G***GGT***TGGGTGTGTGACGG***ACC***
WT-slS3	G***GGT***TGGGTTGTGACGGGC***ACC***

[a]WT is the 89-nucleotide long analyte to represent the 16S rRNA. The abbreviation "S" represents the selective arm, with a short binding sequence that has a temperature of melting (Tm) of 26°C. "U" is the unwinding arm that has a 30-nucleotide analyte-binding arm. T1406A represents the mutant allele on the target, which was used to show the probes can clearly differentiate the wild type from no target present. A stem-loop constraint was added to some of the designs in order to increase selectivity, the designs with this addition are labeled with the letters "sl" and have bolded

and italicized residues to show which sequences form the stem-loop. (Note: Color coordination represents corresponding complementary sequences, expected to anneal. Underlined residues represent single nucleotide substitutions.)

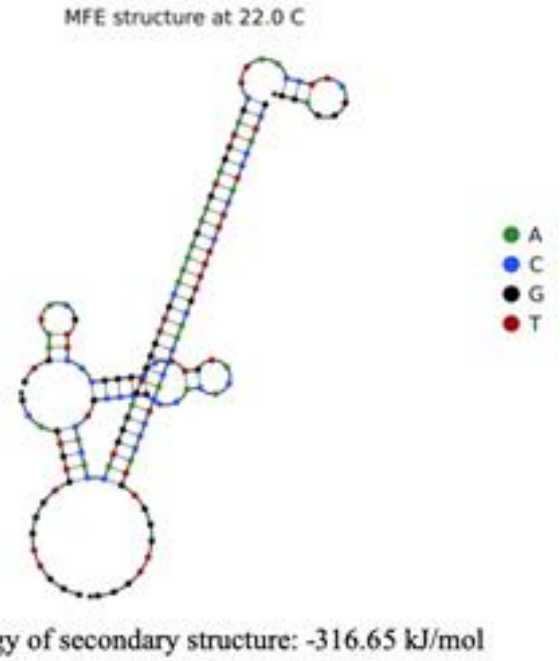

Figure 3: Structure of the complex formed by the sPDz probe with the WT target in the absence of the Blocking Element.

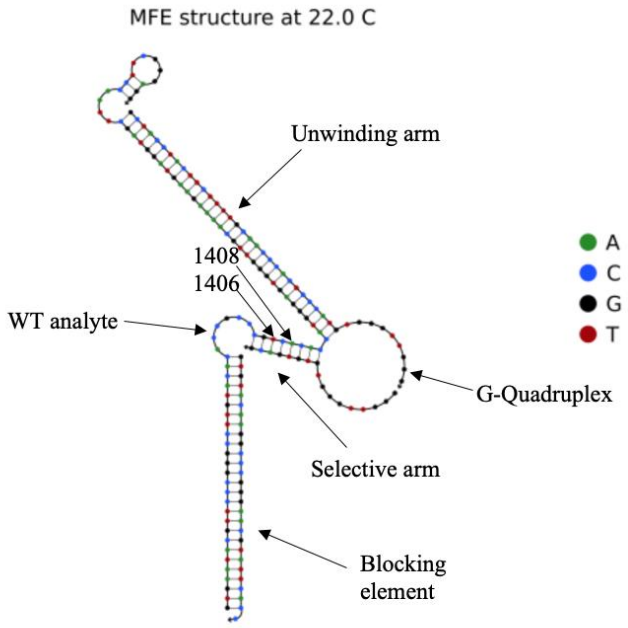

Figure 4: Structure of the complex formed by the sPDz probe with the WT target.

We optimized the following parameters of the sPDz probe: the signal; the selectivity. The signal was measured by the absorbance at 420 nm, subtracted by the background absorbance. The selectivity is the quantitative measure of the difference between the absorbance from the wild type and the absorbance of the mutant. When designed properly, the wild type has high amounts of catalyzation, while the mutant does not. We tested the selectivity of the probe using WT and mutant analytes. The selectivity was measured using the selectivity factor (SF) calculated with Equation 1.

$$SF = 100\% * (1 - (A_M - A_0)/(A_{WT} - A_0))$$

Equation 1: Selectivity Factor

A_M is the average absorbance of the probe triggered by the mismatched target, A_0 is the average absorbance of the No-Target-Control, A_{WT} is the average absorbance of the probe triggered

by the specific target. The probes were only considered effective when the selectivity was greater than 80% but are best when greater than 95%. For example, if the signal triggered by the fully complementary target is low, the analyte-binding arm of strand S can be extended, giving it more complementary regions for binding. Another tool to increase the signal was to introduce a non-nucleotide linker between the G4-forming and analyte-binding fragments of the strands for improved flexibility.[17] If the selectivity is not optimal, the length of the analyte-binding arm of strand S can be reduced, which would decrease the melting temperature of the probe's complex with the mutant analyte. Alternatively, a structural constraint in the form of a stem-loop could be introduced in strand S, as described in Connelly 2019. In this case, a segment on the selective arm can be added that is complementary to a portion of the G4-forming fragment. When introduced into the solution it has to balance between intermolecular (probe binding to the analyte) and intramolecular (probe binding to itself) forces, which will skew the equilibrium, making it so fewer G4 will form when the binding arm is weaker, such as with mutations. The self-complementary loop should not decrease the signal of the wild type significantly, but it significantly increases the selectivity for these conditions.[17]

The sensors were first tested in the absence of Blocking element. This element was designed and added into the experiment to serve the function of making the region of interest more open to the split-G4 probes. The Blocking element has the capabilities of binding with a strong affinity to a region downstream of the mutation site. This affinity was hypothesized to undo the secondary structure of the 16S rRNA to increase the ability of the probes to access the target. A sample was tested under annealing conditions to find the ability of the probe to catalyze the reaction when bound to the target. The annealing conditions have been previously shown to

increase the signal by raising the temperature of the solutions to at 95ºC for five minutes and letting the probes hybridize, forming the most stable conformation.

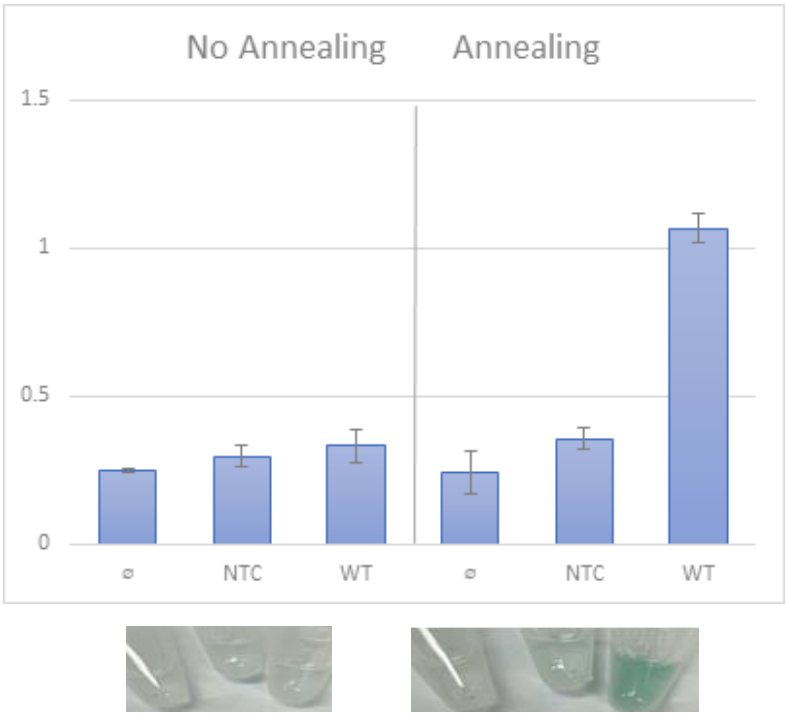

Figure 5: Absorbance at 420 nm without Blocking Element

(Normal conditions on left; Anneal on right.) ⌀ is the blank control sample, only containing the buffer solution and added reagents. NTC is the no target control sample, which contains the buffer, the WT-S1 and WT-U1 probe strands and the added reagents. WT sample contains all the components, the buffer, synthetic probes, WT target, and the added reagents. The three samples on the left were performed without prior annealing of the probe strands to the target. The three samples on the right were performed under annealing conditions. Three trials of each experiment were performed unless no error bars are shown in the figure. The error bars represent the standard deviation of the three trials.

The no-target control (NTC) sample contained WT-S1 and WT-U1 in the absence of the Blocking element and any target in the reaction buffer. The WT condition had the WT target, the WT-S1 and WT-U1, but no Blocking Element. As can be seen from Figure 5, the WT sample

could not be differentiated from the NTC sample without annealing of the probe to the target (left panel). However, with the annealing step, the probes were able to bind to their specific target to form the PDz core to catalyze the reaction and produce a dark-colored product (right panel). This shows that when the probes bind, they can catalyze the desired reaction, but they need help binding to the target.

The samples were not capable of generating a strong enough signal without the Blocking element and/or prior annealing to the target. This is most likely due to the fact that the target has a high secondary structure with itself, preventing hybridization of the probes to the target. Because the samples were not able to give a high signal, a new method needed to be added to help the sensors bind but keep selectivity with the WT and the mutants. The design must have a high affinity to the target to shift the equilibrium and open up the target strands for binding. The Blocking element was designed to accomplish such a task and was added to the next sets to test its ability to do so.

Effect of a Blocking Element

The next sets were prepared in the same methods previously described, but with the addition of the Blocking Element.

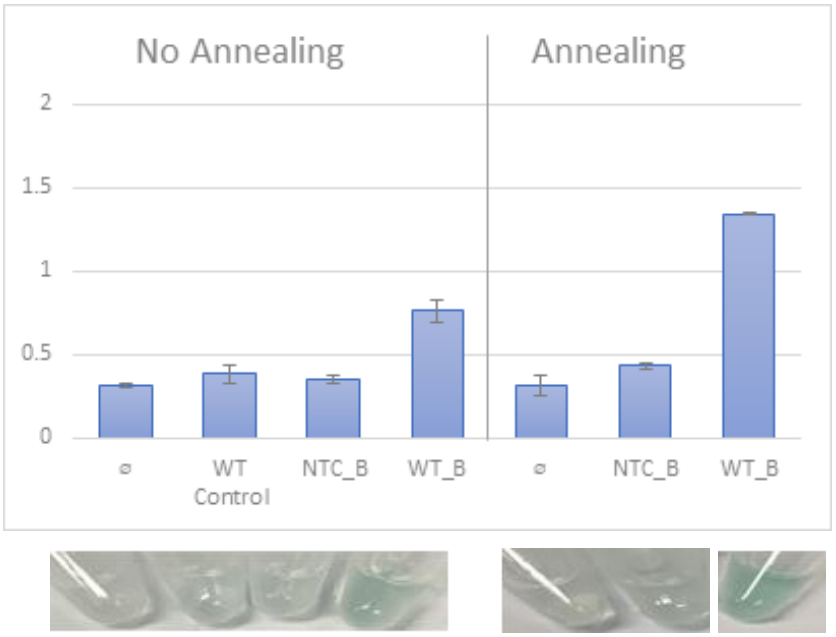

Figure 6: Absorbance at 420 nm of Sets with WT-S1 and WT-U1 without prior annealing (Left) and Anneal (Right) following incubation with reagents.

The "_B" denotation represents the samples that were made in the presence of the Blocking Element. The three samples on the left were measured without prior annealing of the probe strands to the target. The three samples on the right were performed under annealing conditions. The WT Control samples contained the solution with only the reagents and the WT target, but no probes to bind to. This control group was used to ensure the WT target was not catalyzing the reaction on its own.

The results of the assay testing in the presence of the Blocking element without probe-target annealing show the success of the probe to give off signal when binding to the targets (Figure 6, left panel). For these initial samples, a control group called "WT control" was added to ensure that the WT DNA strands by themselves were not catalyzing the reaction. These samples were prepared in the same manner as the negative controls with the addition of 1 μM of the WT target strands alone. Due to the high number of guanine nucleotides in the WT sequence, this test was

performed to confirm that the WT DNA by itself is incapable of forming the G4 and would not catalyze the reaction and invalidate the results. The next sample, labeled WT, was used to measure the ability of the synthetic probes to bind to the WT DNA and catalyze the reaction. The WT sample was prepared the same as the blank control, but with the addition of WT target DNA and the WT-S1 and WT-U1 probes. When comparing the WT sample from Figure 6 to the controls, you can see a differentiation between the two samples. The comparison of the WT with and without the blocking element shows that by adding the blocking element to this solution, the signal increases (compare left panels in Figures 5 and 6).

The annealed set was prepared in the same solutions as the previous set, but under annealing conditions. The WT condition had the WT-S1 and WT-U1 probes and target DNA, so the annealing conditions increased the hybridization of these two entities, resulting in a greater amount of reaction catalyzed and a greater absorbance.

The next set, the incubated set, was also prepared in the same solutions as the normal conditions, but the DNA samples were allowed to incubate together for a minimum of 24 hours at room temperature before adding the reagents and measuring the samples after 15 minutes. This period of 24 hours for incubation was to allow more time for the DNA samples to reach equilibrium of their annealed states.

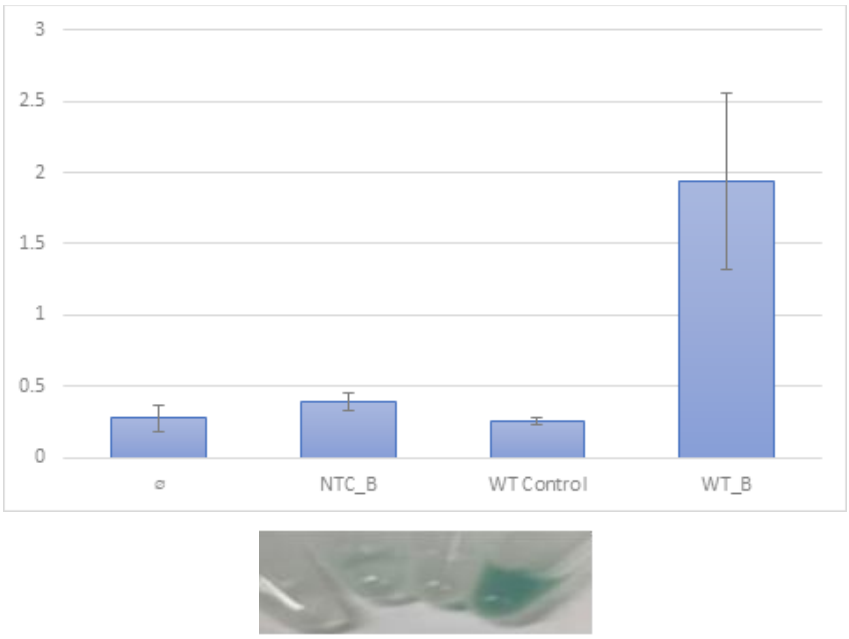

Figure 7: Absorbance at 420 nm of sets following 24 hours of incubation.

⌀ is the blank control sample, only contained the buffer solution and added reagents. NTC is the no target control sample, which contains the buffer, the WT-S1 and WT-U1 probes and the added reagents. The WT Control samples contained the solution with only the reagents and the WT target, but no probes to bind to. This control group was used to ensure the WT target was not catalyzing the reaction on its own. WT sample contains all the components, the buffer, synthetic probes, WT target, and the added reagents.

By observing Figure 7, the WT sample had a strong change in color compared to their respective controls. The conditions of these samples would not be ideal for clinical settings as the results take much longer than the proposed test. This set was merely designed to measure the ability of the probes to bind to the target, and it showed they can bind very strongly.

The last set shown below was done under identical conditions as the normal set, except that the pH of the solution had been changed to a pH of 6.8 from 7.4 (Figure 8). This change in pH was

expected to increase the absorbance for all samples including the NTC sample. By observing Figure 8 and comparing those samples to the samples shown in the left panel of Figure 6 (No annealing), the color change is prominent.

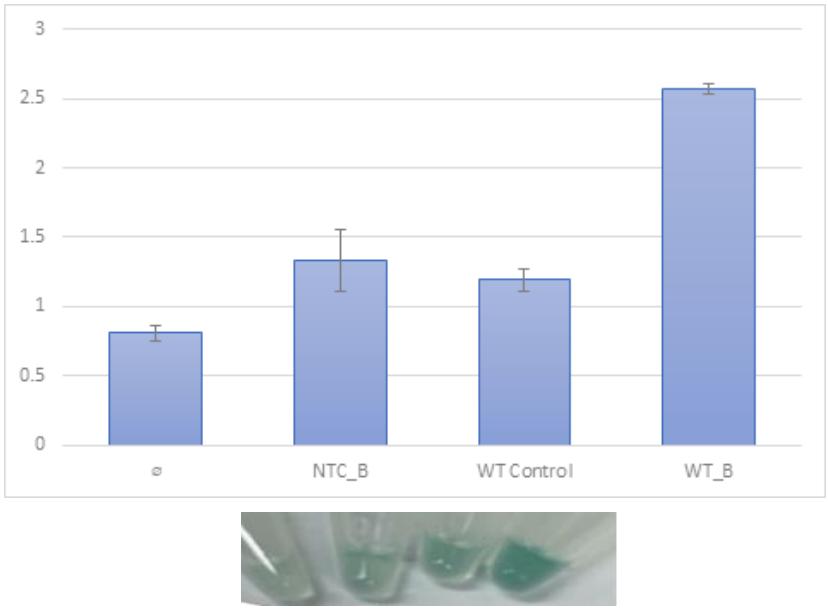

Figure 8: Absorbance at 420 nm of WT-S1 and WT-U1 sets at pH 6.8 following incubation with reagents.

The WT_B sample contained the WT target, Blocking element, the WT-S1 and WT-U1 probes. The WT Control samples contained the solution with only the reagents and the WT target, but no probes to bind to. This control group was used to ensure the WT target was not catalyzing the reaction on its own.

Upon analyzing the all of the above results and further consideration of the WT-S1 selective arm, we concluded that this design will not be selective enough when it comes to the A1408G mutant vs. wild type testing. The 1408 mutation site will be too close to the junction of the G4, so the substitutions could form Wobble base pairs and decrease selectivity. One of the future goals of this project is to test this probe on the A1408G mutation, which lead to the decision that a readjustment was necessary. The subsequent probes were designed by shifting the selective

arm up a small number of nucleotides. The redesigned probes were then tested in similar conditions to learn about the new designs' ability to bind and catalyze the reaction, and the strength of the reaction.

Selectivity of the G4-PDz Probes

The new WT-S2 and WT-U2 probes with an upward shift were tested first, with and without the Blocking Element to learn about its effect on the signal produced. Additionally, a DNA target containing the T1406A mutation, such as the mutation in the 16S ribosomal subunit that is associated with gentamicin resistance was tested. This target will be compared to the signal of the wild type target to analyze the probe's selectivity.

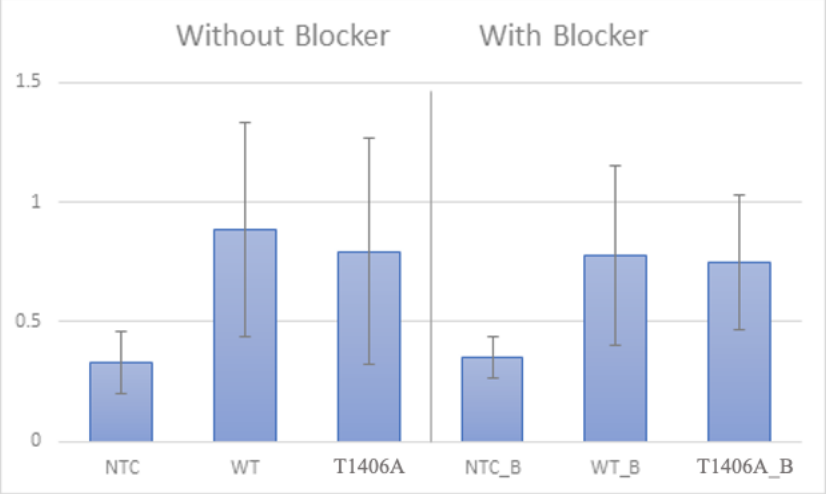

Figure 9: Absorbance at 420 nm of WT-S2 and WT-U2 without Blocking Element (Left) and with Blocking Element (Right) sets following incubation with reagents.

T1406A is the mutant sequence tested that is correlated with gentamicin resistance.

The WT-S2 and WT-U2 samples showed no change in signal in the presence of the Blocking Element compared to the counterparts without the Blocking Element. These samples also experienced a slightly higher background signal than some previous designs, but it remained at a moderate and workable level.

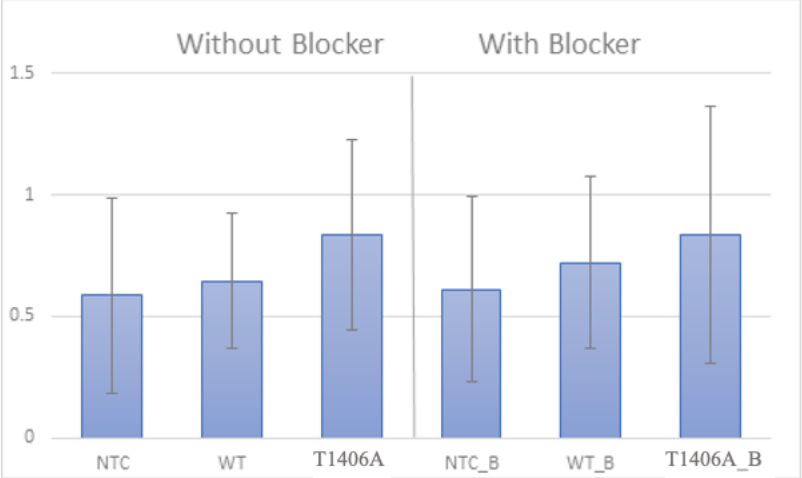

Figure 10: Absorbance at 420 nm of WT-S3 and WT-U3 without Blocking Element (Left) and with Blocking Element (Right) sets following incubation with reagents.

The samples containing the WT-S3 and WT-U3 with and without the Blocking Elements had a high background signal. This can most likely be explained by the samples forming the G4 without being coordinated by binding to a target. The signal was also increased when binding to the T1406A target when compared to the WT, which was the opposite of the intended design.

It was decided that the effect of the blocking element would vary in a case-by-case scenario and that all of the designs would be tested with or without the presence of a blocking element.

The probes with high signal and low background will be the most promising to optimize. Since selectivity can be increased by adding constraints, such as stem-loops, such designs will be added following choosing the most optimal sensors. Because of the low WT to background signal ratio, the S3/U3 designs most likely would not be able to be optimized for the purposes of this experiment. The S1/U1 pair was predicted to be unsuccessful distinguishing mismatches because of the high chance of having wobble base pairs to the substitution. The S2/U2 designs appeared to be the most promising to optimize to the purposes of this experiment. Both the second and third designs, WT-S2/U2 and WT-S3/U3, were modified to contain the addition of a stem-loop constraint intended to increase the selectivity and decrease the background signals.

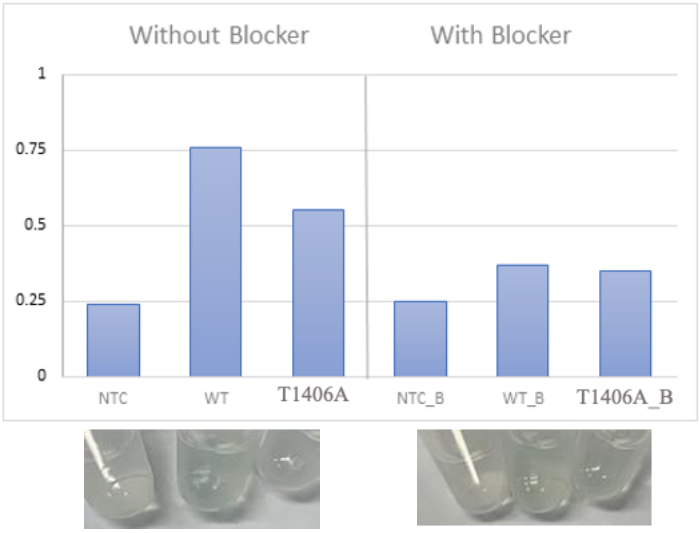

Figure 11: Absorbance at 420 nm of WT-slS2 and WT-U2 without Blocking Element (Left) and with Blocking Element (Right).

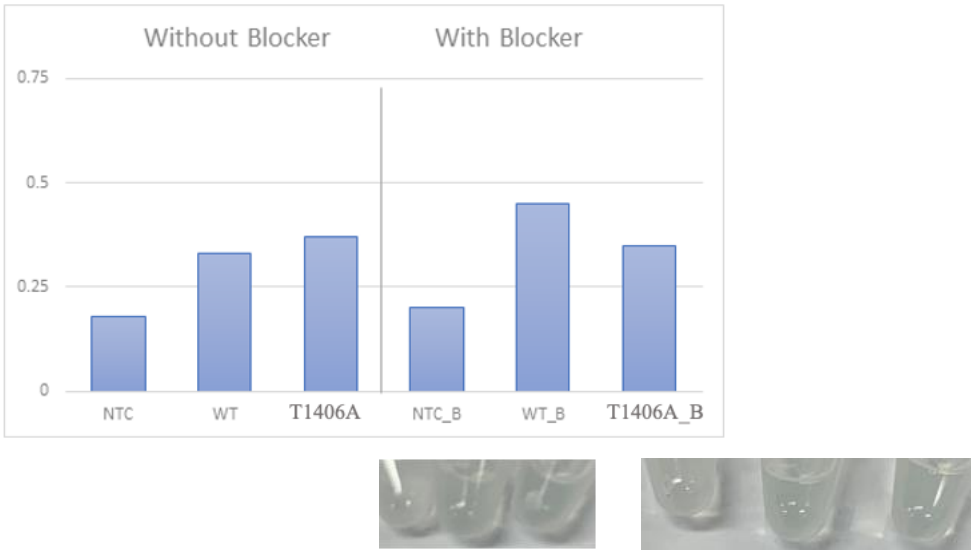

Figure 12: Absorbance at 420 nm of WT-slD2SA-1 and WT-U2 without Blocking Element (Left) and with Blocking Element (Right).

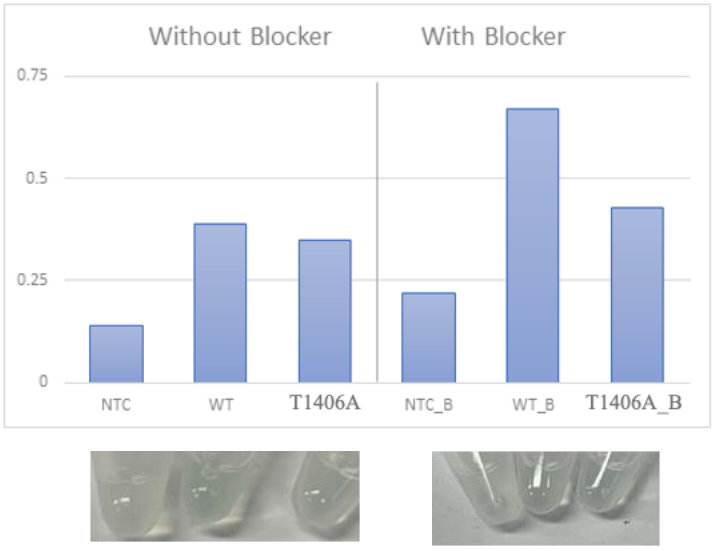

Figure 13: Absorbance at 420 nm of WT-slS3 and WT-U3 without Blocking Element (Left) and with Blocking Element (Right).

The incubation test that allows the probes and target incubate for 24 hours is a great test to understand a probe's potential to produce a signal and be selective. This is because they are given

plenty of time to reach equilibrium before the reagents are added, and this allows the sPDz to be coordinated if it is favorable. The slD2SA-1 and U2 probes were run after 24 hours of incubation with the targets and Blocking Element to see the signal and selectivity once the contents have reached the most stable conformations (Figure 14).

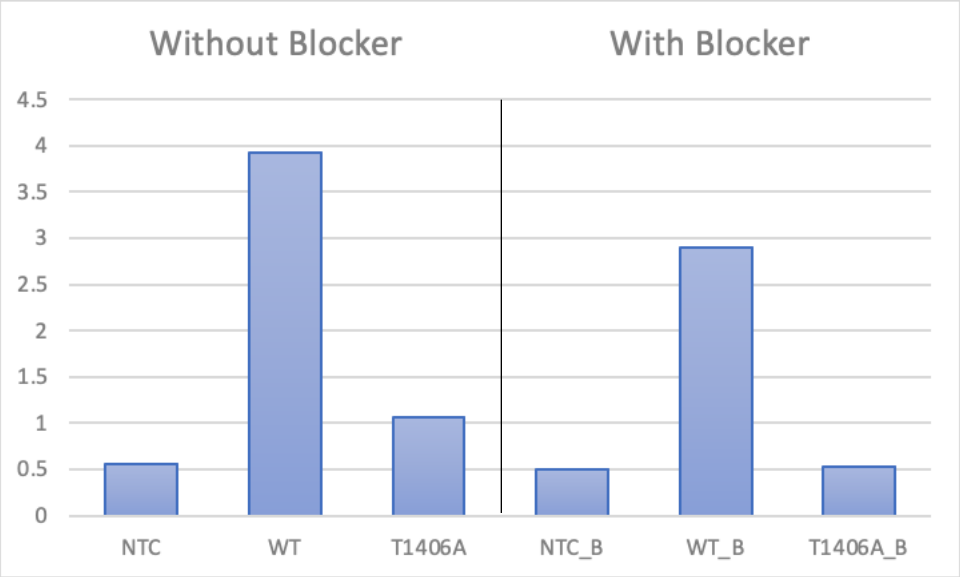

Figure 14: Absorbance at 420 nm for slD2SA-1 probes after 24 hours of incubation at room temperature.

After analyzing the results of the incubation test (Figure 14), and the selectivity of all the probes (Figure 9-13), it was decided that the slD2SA-1 probe in the presence of the Blocking Element was the most promising. It offered the highest signal, with very low background activity, and was selective for the WT target because a small signal was observed in the T1406A target. The Blocking Element appeared to hurt the signal of the probe on the WT target, but it also had a positive effect on the selectivity of this probe. The purpose of the Blocking Element was to improve the probe on the 16S rRNA target, so this probe was then tested on an RNA target in the presence of the Blocking Element, isolated from *E. coli* cells harvested in the lab for preliminary data. This target will be tested without the presence of the Blocking Element in future projects.

Interrogation of Total *E. coli* RNA

Following the methods described in the procedures section, the purified *E. coli* RNA was run in an agarose gel electrophoresis to look for isolation of 16S rRNA. Two samples were obtained from the phenol-chloroform RNA extraction and therefore both samples were run in the gel (Figure 15). The *E. coli* 16S rRNA is 1541 nucleotides long, so we expected to see a band approximately at the same level as the 1500 marker on the ladder. However, we ended up seeing a slight smear that began at that height and ran down until about 200 nucleotides. The reason for this smear was hypothesized to be the partial hydrolysis of the 16S rRNA. Due to time constraints surrounding COVID-19 and social distancing regulations, the colorimetric assay was performed, despite the apparent hydrolysis of the 16S rRNA WT *E. coli* target.

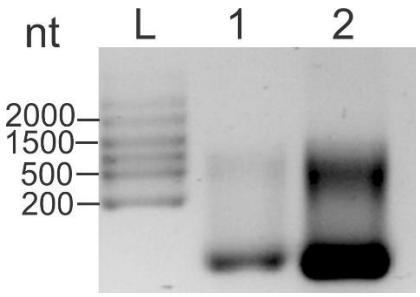

Figure 15: Analysis of samples of total E. coli RNA by 0.8% agarose gel electrophoresis. L – high-range RNA ladder (size of the RNA markers are indicated next to the corresponding bands). Lanes 1 and 2 contain two different preparations of total RNA isolated from *E. coli* cells.

The concentration was first calculated on the GelDoc by measuring the intensity of the band in the sample lanes and comparing them to that of the RiboRuler High-Range RNA Ladder. It was estimated that there was 6,234.2 ng of 16S rRNA in the 18.5 µL sample. If all 6,234.2 ng

of 16S rRNA precipitated then the target was at a concentration of roughly 1.19 µM; however, it is unknown how much of the 16S rRNA was lost.

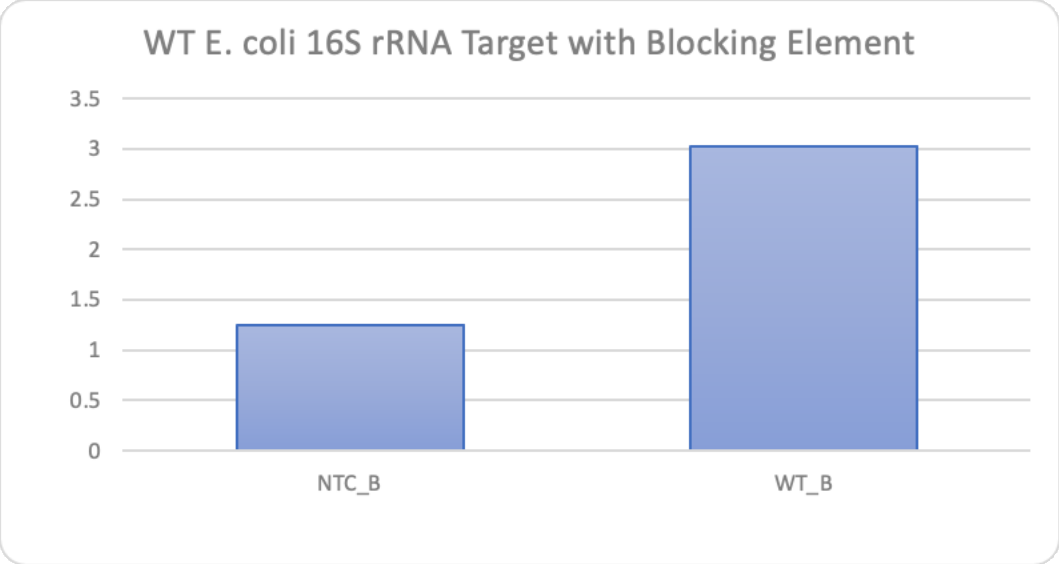

Figure 16: WT *E. coli* 16S rRNA Target with slD2SA-1 and U2 Probes.

Only one trial was performed with the 16S rRNA *E. coli* target in the presence of the slD2SA-1 probe, however this trial showed promising results. The probes were still able to bind to the target and generate a signal, despite the complex structure of the WT target. The probes were not tested in the presence of a mutant 16S rRNA target because of the resistance to gentamicin, but there is no reason to believe the probes would generate more signal on this target than on the T1406A mutant DNA target, which would grant the probe enough selectivity to be ideal in clinical settings.

DISCUSSION

Currently, this publication outlines the use of targeting gentamicin resistance from mutations in nt 1406 of the 16S rRNA in *E. coli* cells and their presence in the solution for optimal diagnostics. Gentamicin resistance is also linked to mutations in the 1408 nucleotide of the 16S rRNA in *E. coli*.[7] Future plans of this laboratory are to test the probes on the A1408G mutation on synthetic targets as well as the WT *E. coli* 16S rRNA without the presence of the Blocking element. Other future plans are to develop similar mechanisms for detection of point mutations conferring other kinds of antibiotic resistance in bacteria to be used quickly, easily, and efficiently to make for enhanced clinical diagnosis and treatment. Another future goal is to develop a mutant-specific probe, which can bind to the mutant targets to generate a signal, and when used in parallel with the WT specific probes can distinguish between the presence and absence of *E. coli*, necessary for UTI diagnostics. A final goal for this project would be to test the final probes on gentamicin resistant *E. coli* to confirm the selectivity of the probes on live cells, not just synthetic targets.

Following further trials of the split-G4 probes on *E. coli* total RNA (Figure 16), the probes should be tested on varying concentrations of *E. coli* RNA to validate the probes' signal. By varying the concentrations of *E. coli* RNA, we will show how dilute the samples can be and still be useful for diagnosis.

Following the successful testing of the probes on *E. coli* RNA, the probes should be tested using artificial urine spiked with *E. coli* cells. The artificial urine sample would contain compounds that are commonly found in urine, such as urea, potassium, etc.[20] A bacteriological

filter could be used to filter the urine, which has a diameter between 0.5-5 μm. Using such a filter, or centrifuge to create a pellet, can isolate the *E. coli* cells, thereby increasing the concentration of rRNA in the solution we were targeting to run the reaction. The signal and selectivity could then be calculated and analyzed for significance. RNA purification can be a long and tedious process, which ideally should be bypassed to optimize expedient results. In order to show you can skip having to purify total cellular RNA for diagnostics, the probes should be tested on *E. coli* lysates after performing serial dilutions. However, it may not be optimal to use lysates because of the presence of nucleases, which would break down the targets or probes, peroxidases, which would indicate false positives, and other cellular components.

The presence of the Blocking Element had no significant changes on formation of the G4 compared to the samples that did not have this element. Additionally, it was thought that when the stem-loop constraints are designed that in some cases the blocking element would block the selective arm from binding. This would happen if the stem-loop portion hybridized somewhere downstream without the presence of the blocking element, which would stabilize the structure. In the presence of the blocking element, it may prevent that binding and the selective arm will be less likely to bind. In other cases, the blocking element may help under the secondary structures of the target, to make it easier for the binding arms of the G4 to bind. In some of the cases, the Blocking Element hurt the signal or the selectivity factor, in other cases these values were positively affected, and in some cases, there was no significant affect. Due to this variability, we suggest that all samples and probes be tested with and without the presence of the Blocking Element to find the most optimal conditions.

REFERENCES

1. Behzadi, P., Behzadi, E., Yazdanbod, H., Aghapour, R., Akbari Cheshmeh, M., & Salehian Omran, D. (2010). A survey on urinary tract infections associated with the three most common uropathogenic bacteria. Maedica, 5(2), 111–115.
2. Becknell, B., Schober, M., Korbel, L., & Spencer, J. D. (2015). The diagnosis, evaluation and treatment of acute and recurrent pediatric urinary tract infections. Expert review of anti-infective therapy, 13(1), 81–90. https://doi.org/10.1586/14787210.2015.986097
3. Simmering, J. E., Tang, F., Cavanaugh, J. E., Polgreen, L. A., & Polgreen, P. M. (2017). The Increase in Hospitalizations for Urinary Tract Infections and the Associated Costs in the United States, 1998-2011. Open forum infectious diseases, 4(1), ofw281. https://doi.org/10.1093/ofid/ofw281
4. Flores-Mireles, A. L., Walker, J. N., Caparon, M., & Hultgren, S. J. (2015). Urinary tract infections: epidemiology, mechanisms of infection and treatment options. Nature reviews. Microbiology, 13(5), 269–284. https://doi.org/10.1038/nrmicro3432
5. Schmiemann, G., Kniehl, E., Gebhardt, K., Matejczyk, M. M., & Hummers-Pradier, E. (2010). The diagnosis of urinary tract infection: a systematic review. Deutsches Arzteblatt international, 107(21), 361–367. https://doi.org/10.3238/arztebl.2010.0361
6. Labovitz, E et al. “Single-dose daily gentamicin therapy in urinary tract infection.” Antimicrobial agents and chemotherapy vol. 6,4 (1974): 465-70. doi:10.1128/aac.6.4.465

7. Holbrook, Selina Y L, and Sylvie Garneau-Tsodikova. “Evaluation of Aminoglycoside and Carbapenem Resistance in a Collection of Drug-Resistant Pseudomonas aeruginosa Clinical Isolates.” *Microbial drug resistance (Larchmont, N.Y.)* vol. 24,7 (2018): 1020-1030. doi:10.1089/mdr.2017.0101
8. Recht, M I, and J D Puglisi. “Aminoglycoside resistance with homogeneous and heterogeneous populations of antibiotic-resistant ribosomes.” Antimicrobial agents and chemotherapy vol. 45,9 (2001): 2414-9. doi:10.1128/aac.45.9.2414-2419.2001
9. Hasvold, J., Bradford, L., Nelson, C., Harrison, C., Attar, M., & Stillwell, T. (2013). Gentamicin resistance among Escherichia coli strains isolated in neonatal sepsis. Journal of neonatal-perinatal medicine, 6(2), 173–177. https://doi.org/10.3233/NPM-1365512
10. Zankari, E., Allesøe, R., Joensen, K. G., Cavaco, L. M., Lund, O., & Aarestrup, F. M. (2017). PointFinder: a novel web tool for WGS-based detection of antimicrobial resistance associated with chromosomal point mutations in bacterial pathogens. The Journal of antimicrobial chemotherapy, 72(10), 2764–2768. https://doi.org/10.1093/jac/dkx217
11. Mahdieh, N., & Rabbani, B. (2013). An overview of mutation detection methods in genetic disorders. Iranian journal of pediatrics, 23(4), 375–388.
12. Deekshit, V. K., Jazeela, K., Chakraborty, G., Rohit, A., Chakraborty, A., & Karunasagar, I. (2019). Mismatch amplification mutation assay-polymerase chain reaction: A method of detecting fluoroquinolone resistance mechanism in bacterial pathogens. *The Indian journal of medical research*, *149*(2), 146–150. https://doi.org/10.4103/ijmr.IJMR_2091_17
13. Wood, H. N., Sidders, A. E., Brumsey, L. E., Morozkin, E. S., Gerasimova, Y. V., & Rohde, K. H. (2019). Species Typing of Nontuberculous Mycobacteria by Use of

Deoxyribozyme Sensors. Clinical chemistry, 65(2), 333–341. https://doi.org/10.1373/clinchem.2018.295212

14. Reed AJ, Connelly RP, Williams A, et al. Label-Free Pathogen Detection by a Deoxyribozyme Cascade with Visual Signal Readout. Sensors and actuators. B, Chemical. 2019 Mar;282:945-951. DOI: 10.1016/j.snb.2018.11.147.
15. Deng, M., Feng, S., Luo, F., Wang, S., Sun, X., Zhou, X., & Zhang, X. L. (2012). Visual detection of rpoB mutations in rifampin-resistant Mycobacterium tuberculosis strains by use of an asymmetrically split peroxidase DNAzyme. Journal of clinical microbiology, 50(11), 3443–3450. https://doi.org/10.1128/JCM.01292-12
16. Kolpashchikov D. M. (2008). Split DNA enzyme for visual single nucleotide polymorphism typing. Journal of the American Chemical Society, 130(10), 2934–2935. https://doi.org/10.1021/ja711192e
17. Connelly, R. P., Verduzco, C., Farnell, S., Yishay, T., & Gerasimova, Y. V. (2019) Toward a Rational Approach to Design Split G-Quadruplex Probes. ACS chemical biology, 14(12), 2701–2712. DOI: 10.1021/acschembio.9b00634
18. Li, W., Li, Y., Liu, Z., Lin, B., Yi, H., Xu, F., Nie, Z., & Yao, S. (2016). Insight into G-quadruplex-hemin DNAzyme/RNAzyme: adjacent adenine as the intramolecular species for remarkable enhancement of enzymatic activity. Nucleic acids research, 44(15), 7373–7384. https://doi.org/10.1093/nar/gkw634
19. Zadeh, J. N., Steenberg, C. D., Bois, J. S., Wolfe, B. R., Pierce, M. B., Khan, A. R., Dirks, R. M., and Pierce, N. A. (2011) NUPACK: Analysis and design of nucleic acid systems. J. Comput. Chem. 32, 170−173.

20. Bouatra, S., Aziat, F., Mandal, R., Guo, A. C., Wilson, M. R., Knox, C., Bjorndahl, T. C., Krishnamurthy, R., Saleem, F., Liu, P., Dame, Z. T., Poelzer, J., Huynh, J., Yallou, F. S., Psychogios, N., Dong, E., Bogumil, R., Roehring, C., & Wishart, D. S. (2013). The human urine metabolome. *PloS one*, *8*(9), e73076. https://doi.org/10.1371/journal.pone.0073076